Molecular Biology of the Cell
Vol. 15, 132–141, January 2004

Lipid-dependent Bidirectional Traffic of Apolipoprotein B in Polarized Enterocytes

Etienne Morel, Sylvie Demignot, Danielle Chateau, Jean Chambaz, Monique Rousset, and François Delers*

Unité Mixte de Recherche, Institut National de la Santé et de la Recherche Médicale U505, Université Pierre et Marie Curie, Laboratoire de Pharmacologie Cellulaire et Moléculaire de l'EPHE, 75006 Paris, France

Submitted April 8, 2003; Revised September 19, 2003; Accepted September 19, 2003
Monitoring Editor: Randy Schekman

Enterocytes are highly polarized cells that transfer nutrients across the intestinal epithelium from the apical to the basolateral pole. Apolipoprotein B (apoB) is a secretory protein that plays a key role in the transepithelial transport of dietary fatty acids as triacylglycerol. The evaluation of the control of apoB traffic by lipids is therefore of particular interest. To get a dynamic insight into this process, we used the enterocytic Caco-2 cells cultured on microporous filters, a system in which the apical and basal compartments can be delimited. Combining biochemical and morphological approaches, our results showed that, besides their role in protection from degradation, lipids control the intracellular traffic of apoB in enterocytes. A supply of fatty acids and cholesterol is sufficient for the export of apoB from the endoplasmic reticulum and its post-Golgi traffic up to the apical brush-border domain, where it remains until an apical supply of complex lipid micelles signals its chase down to the basolateral secretory domain. This downward traffic of apoB involves a microtubule-dependent process. Our results demonstrate an enterocyte-specific bidirectional process for the lipid-dependent traffic of a secretory protein.

INTRODUCTION

The intracellular traffic of proteins has been extensively studied in the past few years (Harter and Reinhard, 2000; Kirchhausen, 2000; Lippincott-Schwartz *et al*., 2000; Nelson and Yeaman, 2001). Numerous partners that control the formation of carrier vesicles at the various stages in this intracellular transport process (Nickel *et al*., 1998; Kirchhausen, 2000) as well as several sorting motifs determining the specific targeting for apical and basolateral membrane proteins in polarized epithelial cells (Keller and Simons, 1997; Nelson and Yeaman, 2001) have been described. The influence of lipids on the functional properties of the vesicular compartments involved in protein traffic has also provoked increasing interest (McMaster, 2001; Nelson and Yeaman, 2001).

Enterocytes are highly polarized absorptive cells (Massey-Harroche, 2000) responsible for the transepithelial transfer of nutrients from the luminal side of the intestine to the bloodstream. This transepithelial transfer depends on the efficient sorting and targeting of specialized proteins. Studies on the polarized traffic of proteins in enterocytes have therefore focused on specialized membrane proteins present in the apical brush border or in the basolateral plasma membrane (Hauri *et al*., 1985; Hauri, 1988; Lestavel and Fruchart, 1994; Abumrad *et al*., 1999; Jacob and Naim, 2001; Naim, 2001). By contrast, the traffic of secretory proteins in enterocytes, although vital for intestinal function, still remains poorly documented.

Study of the traffic of apolipoprotein B (apoB) in enterocytes is of particular interest because apoB is a secreted protein and may be subject to regulation by lipids. apoB is a major structural component of triacylglycerol-rich lipoproteins (TRLs) and a key element in the trans-epithelial transport of dietary fatty acids as triacylglycerol (TAG) (Davidson and Shelness, 2000). Almost all of the studies on the processing and stability of apoB were carried out in the liver (Fisher *et al*., 1997; Yao *et al*., 1997; Carpentier *et al*., 2002; Fisher and Ginsberg, 2002), the other site of TRL production. In hepatocytes, a reduced supply of fatty acids was found to promote apoB proteolysis (Davidson and Shelness, 2000). By contrast, a large pool of intracellular apoB was reported to persist in the absence of an exogenous supply of fatty acids in the enterocytic Caco-2 cells (Liao and Chan, 2000), the in vitro model for the study of the enterocytic transfer of nutrients (Delie and Rubas, 1997; Hussain *et al*., 2001). This was also reported in fructose-fed hamster enterocytes, though some apoB degradation was observed in this model (Haidari *et al*., 2002).

The small intestine is subject to major fluctuations in luminal lipid content that could influence the location of apoB in the intestinal mucosa: apoB was found localized in Golgi cisternae and vesicles in human absorptive intestinal cells after a fat meal (Christensen *et al*., 1983), but the presence of apoB in Golgi cisternae of enterocytes was also

Article published online ahead of print. Mol. Biol. Cell 10.1091/mbc.E03–04–0215. Article and publication date are available at www.molbiolcell.org/cgi/doi/10.1091/mbc.E03–04–0215.

* Corresponding author. E-mail address: fransisco.delers-u505@bhdc.jussieu.fr.

Abbreviations used: apoB, apolipoprotein B; BBD brush border domain; BSA, bovine serum albumin; CHX, cycloheximide; FA, fatty acid; FCS, fetal calf serum; FITC, fluorescein isothiocyanate; ITS, insulin transferrin selenium; ITS/L, insulin transferrin selenium and lipids; MTP, microsomal transfer protein; SAC, subapical compartment; SI, sucrase-isomaltase; TAG, triacylglycerol; TGN, *trans*-Golgi network; TRL, triacylglycerol-rich lipoprotein; WGA, wheat germ agglutinin.

reported in fasted rats (Levy *et al*., 2002). Earlier immunofluorescence studies have reported an apical localization of apoB in epithelial intestinal cells of bile-diverted fasted rats but not in animals that were only fasted (Glickman *et al*., 1976). In human fetal enterocytes, apoB has been reported to display an apical distribution (Levy and Bendayan, 2000), but a fat meal was reported to abolish the small amount (<10%) of apoB released apically by pig intestinal explants (Danielsen *et al*., 1993). These data, though inconclusive concerning the lipid-dependent subcellular distribution of apoB in enterocytes, underline that enterocytes and hepatocytes may promote different mechanisms of apoB processing, stabilization, and intracellular traffic to achieve their specific metabolic functions. Therefore, the aim of our study, by using polarized enterocytic Caco-2 cells, was to get a dynamic insight into the effect of lipids on the apoB traffic and targeting in enterocytes.

MATERIALS AND METHODS

Materials

Unless indicated, all chemicals were purchased from Sigma (Saint-Quentin-Fallavier, France). Nile Red and C12 Bodipy were purchased from Molecular Probes (Leiden, The Netherlands). [1-^{14}C]-Labeled oleic acid was purchased from ICN (Orsay, France) and [^{35}S]methionine/cysteine mix from PerkinElmer-Cetus, Courtaboeuf, France). We used goat polyclonal anti-apoB antibodies (Immuno France, Illkirch, France), mouse monoclonal anti-apoB antibodies 2E3 and 5F8 (Monosan, Tebu, Le Perray en Yvelines, France), the anti-β-COP antibody against aa 701–715 (Sigma), anti-Golgin 97 antibody (Molecular Probes), rabbit polyclonal anti-human *Zonula occludens* (ZO1) antibodies (Zymed Laboratories, South San Francisco, CA), anti-protein disulfide isomerase (PDI) antibody (Alexis Biochemical, Lausen, Switzerland), and rabbit polyclonal anti-apoB antibodies, kindly provided by Dr. Mazur. Anti-sec 13p and rabbit polyclonal anti-sucrase-isomaltase L459 antibodies were obtained from Drs. B.L. Tang and A. Zweibaum, respectively. Rabbit polyclonal anti-human microsomal triacylglycerol transfer protein (MTP) antibodies were a generous gift from Dr. C. Shoulders. Fluorescein isothiocyanate (FITC)-labeled lectin from *Triticum vulgaris* (wheat germ aglutinin, WGA) was provided by Molecular Probes. Secondary CY2-, CY3-, and CY5-labeled antibodies were from Jackson ImmunoResearch Laboratories (West Grove, CA). Peroxidase-conjugated goat anti-rabbit immunoglobulins were from Biosys (Compiègne, France).

Methods

Cell Culture. Caco-2 cells were routinely cultured in DMEM (25 mM glucose and glutamax) from Invitrogen (Cergy Pontoise, France) supplemented with 20% heat-inactivated fetal calf serum (Abcys, Paris, France), 1% nonessential amino acids (Invitrogen), penicillin (100 IU/ml), and streptomycin (10 μg/ml) (Invitrogen), maintained under a 10% CO_2/90% air atmosphere at 37°C. Cells were seeded on microporous (1-μm pore size) polyethylene terephtalate (PET) membranes (Falcon; BD Biosciences, Meylan, France) at a density of 150×10^3 cells/cm^2. The medium was changed in both compartments after 2 d and daily thereafter. After confluence, cells were maintained in culture for 2 wk but a serum-free medium was used in the upper compartment. In some experiments, the cells were seeded on filters in the presence of complete medium for 48 h and were then cultured in DMEM in which serum had been replaced by 1× insulin transferrin selenium (ITS)-mix (Invitrogen; 10 μg/ml insulin, 0.55 μg/ml transferrin, and 6.7 ng/ml selenium). In some experiments, the ITS medium in the lower compartment was supplemented with lipids (0.4 mM oleic acid, 0.2 mM palmitic acid, and 0.04 mM cholesterol) complexed with 1% (wt/vol) fatty acid-free bovine serum albumin with a 4:1 M ratio of fatty acids to albumin (ITS/L). Cell lysates were prepared by rinsing cell layers twice with ice-cold phosphate-buffered saline (PBS) (2.7 mM KCl, 137 mM NaCl in 10 mM phosphate buffer, pH 7.5), scraping the cells into 0.5 ml of 1% (vol/vol) Triton X-100, 5 mM EDTA, and 2% of a protease inhibitor cocktail in PBS, freezing, and storing at −20°C until analysis.

Preparation of Media Supplemented with Micelles. Lipids were added to the apical medium in the form of a complex lipid emulsion, the composition of which was similar to that of the duodenal micelles resulting from lipid digestion (Hernell *et al*., 1990), i.e., 0.6 mM oleic acid, 0.2 mM lysophosphatidylcholine, 0.05 mM cholesterol, 0.2 mM 2-monooleylglycerol, and 2 mM taurocholic acid. When required, 2 μCi of [1-^{14}C] oleic acid (56 mCi/mmol, ICN) per ml final volume of medium or fluorescent Bodipy fatty acid (10 μM) were added. Freshly prepared micellar oleic acid or Bodipy-containing medium was added to the upper compartment, and the cells were incubated for various periods.

Analysis of Lipid Synthesis. Lipids were extracted from cell lysates (100 μl made up to 1 ml with serum-free medium) in 5 ml of chloroform:methanol [2:1 (vol/vol)], and after evaporation, recovered in 75 μl of chloroform: methanol. Aliquots were used for liquid scintillation counting and thin-layer chromatography on Whatman silica-gel plates (Poly-Labo, Strasbourg, France) by using hexane:diethyl-ether:acetic acid [80:20:2 (vol/vol/vol)]. After autoradiography, the radioactive bands were excised and counted in Optiphase Highsafe 2 scintillation fluid (PerkinElmer Wallac, Courtaboeuf, France) in a scintillation counter (Beckman, Gagny, France).

Western Blot Analysis. Protein concentrations were determined with the DC protein assay (Bio-Rad, Marnes la Coquette, France). Aliquots of cell lysates containing 40 μg of proteins were boiled for 4 min with a 1/3 volume of Laemmli buffer (125 mM Tris-HCl, pH 6.8, 4% SDS, 20% glycerol, 0.004% bromphenol blue, 10% 2-mercaptoethanol) and electrophoresed under reducing conditions in a 6% polyacrylamide gel. Proteins were transferred onto Bio-Rad nitrocellulose membranes, which were probed with rabbit polyclonal anti-apoB antibodies and peroxidase-conjugated goat anti-rabbit immunoglobulins and developed using ECL Western blotting reagents according to the manufacturer's instructions (Amersham Biosciences, Orsay, France).

Pulse-Chase Analysis. After incubation for 30 min in a Cys/Met-free medium (Invitrogen), cells were pulsed for 1 h in Cys/Met-free medium supplemented with 150 μCi/ml [^{35}S]Cys/Met in the apical compartment and in the presence or not of lipid micelles. After the pulse, cells were rinsed then chased, for up to 3 h, in the presence of an excess of unlabeled methionine (10 mM) and cystine (2 mM) in both compartments, and in the presence or not of lipid micelles in the apical one. Cell lysates were prepared as described above and centrifuged to remove cell debris. Basolateral media were collected and adjusted to 2% of protease inhibitors cocktail. To be in similar conditions for immunoprecipitation, as far as fetal calf serum (FCS) apoB content is concerned, ITS and ITS/L culture media were supplemented with FCS (20% final concentration). For each sample to immunoprecipitate, 40 μl of a 30% suspension of protein A-Sepharose beads (Amersham Biosciences) in buffer 1 (1% bovine serum albumin [BSA], 0.1% sodium azide in 0.1 M sodium phosphate buffer, pH 8) were incubated for 2 h at room temperature with 200 μl of rabbit polyclonal anti-apoB antibodies (1/100 in the same buffer). The beads were washed twice in buffer 1, once in buffer 2 (0.2% BSA, 1% Triton X-100, 0.1% sodium azide in 0.1 M sodium phosphate buffer, pH 8) and then 200 μl of cell lysate containing 200 μg of proteins, or 250 μl of basolateral media, was added. After 90-min incubation at 4°C, the beads were washed four times with buffer 2, twice with 0.1 M phosphate buffer, pH 8, and once with 10 mM phosphate buffer, pH 8. The beads were boiled for 4 min in 50 μl of Laemmli buffer. Aliquots were counted in Optiphase Highsafe 2 scintillation fluid in a scintillation counter (Beckman) and also subjected to electrophoresis and fluorography to visualize and quantify both apoB isoforms.

Confocal Fluorescence Microscopy. Cells on filters were washed twice with PBS containing 1 mM $CaCl_2$ and 0.5 mM $MgCl_2$, and fixed for 30 min with 4% paraformaldehyde (wt/vol) in PBS at 4°C. After an extensive washing in 150 mM glycine in PBS (PBS-glycine), the cells were permeabilized by incubation for 30 min with 0.1% Triton X-100 in PBS and washed in PBS-glycine followed by PBS plus 1% BSA. Frozen sections of the cell monolayers were prepared by embedding pieces of filter in Tissue-Tek (DAKO, Trappes, France), briefly immersing them in precooled isopentane on liquid nitrogen, and then storing them at −80°C until cutting. Frozen sections were layered onto microscope slides and fixed in 4% paraformaldehyde in PBS. In all conditions, cells were briefly washed in PBS containing 1% BSA and incubated for 60 min with primary antibodies in PBS supplemented with 1% BSA at room temperature and then washed with PBS (4 × 10 min) and stained with secondary antibodies in PBS with 1% BSA for 60 min at room temperature in the dark. After extensive washing in PBS, cells were fixed again in 4% paraformaldehyde in PBS for 10 min, washed twice in PBS, mounted in Fluoprep (BioMérieux, Marcy l'Etoile, France), and examined by confocal fluorescence microscopy (LSM 510 microscope; Carl Zeiss, Jena, Germany). The nature and distribution of the lipids accumulating in Caco-2 cells after lipid absorption were analyzed by Nile Red staining. For biotin labeling, cells were washed with PBS twice and then incubated for 30 min on ice with PBS containing 1 mM $CaCl_2$ and 0.5 mM $MgCl_2$ supplemented with sulfo-NHS-Biotin (Pierce Chemical, Rockford, IL). Any unfixed reagent was inactivated by incubation for 30 min on ice with 200 mM glycine in PBS. Cells were then fixed and permeabilized as described above and biotinylated proteins were detected using 1 μg/ml tetramethylrhodamine B isothiocyanate-labeled streptavidin in PBS.

Electron Microscopy. For apoB immunoelectron microscopy analyses, cells on filters were rinsed with 0.1 M phosphate buffer, pH 7.4 (PB), fixed in 4% paraformaldehyde, 0.1% glutaraldehyde in PB for 60 min, rinsed with PB and 50 mM glycine in PB, and then soaked in 10% gelatin at 37°C for 15 min. Filters were incubated at 4°C and cut into small pieces, which were soaked in 2.3 M sucrose in PB, placed on aluminum holders, and then frozen in liquid

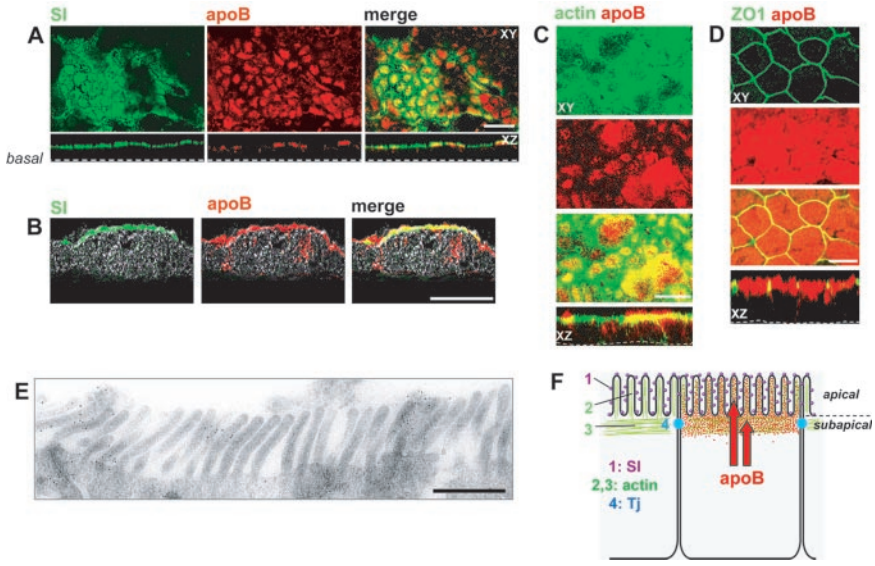

Figure 1. Apical localization of apoB in Caco-2 cells. (A) Immunolocalization of apolipoprotein B (apoB, red channel) and sucrase-isomaltase (SI, green channel) in differentiated Caco-2 cells cultured on filters; top panels represent XY acquisitions at the apical level. Bottom panels show the corresponding XZ projections (bar, 20 μm). (B) Immunolocalization of apoB (red channel) and SI (green channel) on transverse cryosections of Caco-2 cells cultured as in A. Bar, 10 μm. (C) Immunolocalization of apoB (red channel) and phalloidin-FITC labeling of the F-actin network (green channel): top panels represent XY acquisitions at the apical level, and bottom panels show the corresponding XZ projections. Bar, 10 μm. (D) Immunolocalization of apoB (red channel) and ZO1 (green channel); top panels represent XY acquisition at the tight junctions (Tj) plane. Bottom panels show the corresponding XZ projections. Bar, 10 μm. (E) Immunoelectron microscopy analysis of apoB in the BBD of Caco-2 cells. Bar, 1 μm. (F) Schematic representation of the distribution of apoB with respect to markers.

nitrogen. Sections were done at −110°C, placed on grids, washed in buffer A (0.3 M NaCl, 0.5% BSA in PB), and incubated for 15 min with 1% of preimmune goat serum diluted in buffer A to block nonspecific binding. Sections were then incubated with goat polyclonal anti-apoB antibodies for 60 min, rinsed with buffer A, and then with 20 mM Tris, pH 8.4, 0.3 M NaCl, 0.5% BSA (buffer B). They were then incubated with donkey anti-goat antibodies coupled to gold particles (12 nm; Jackson ImmunoResearch Laboratories) for 30 min. Sections were washed, fixed in 1% glutaraldehyde, stained with 2% osmium tetroxide, and after dehydration, embedded in 2% Epon and stained with 0.1% uranyl acetate. For lipids coloration analyses, cells were fixed by 1.5% glutaraldehyde (TAAB Laboratories Equipment, Aldermaston, United Kingdom) in a 0.1 M cacodylate, pH 7.4, buffer during 2 h at room temperature and then placed for 30 min in a 0.2 M imidazole, pH 7.5, buffer containing 4% aqueous osmium tetroxide (Carlo Erba, Val deReuil, France). Cells were then washed for 10 min in a 0.1 M imidazole buffer before dehydration and inclusion in Epon. Ultra thin sections were contrasted with lead citrate for 1 min. Grids were examined in an electron microscope (JOEL, Tokyo, Japan).

RESULTS

apoB Is Apically Localized in Differentiated Caco-2 Cells

Confocal microscopy analysis was used to localize apoB in Caco-2 cells that had been cultured for 21 d on filters in the presence of serum, which was added to the basal compartment. Most of the apoB was apically distributed and colocalized with the brush-border marker sucrase-isomaltase (SI), indicating that part of the apical apoB was located within the microvilli (Figure 1A). Similar results were obtained with cryostat sections of the cell monolayer (Figure 1B), indicating that the observed apical distribution did not result from insufficient permeabilization of the cells. apoB also colocalized with F-actin (Figure 1C), in both the brush-border microvilli and a subapical compartment corresponding to the terminal web. These two domains are delimited by the tight junctions, here visualized with ZO1 (Figure 1D). apoB staining was also observed around the nucleus, although it was much fainter in this region (see Figure 2, −6 μm). The presence of apoB in the brush-border domain (BBD) was confirmed by immunoelectron microscopy (Figure 1E).

Apical apoB Is Derived from the trans*-Golgi Network (TGN)*

To further characterize the subcellular compartments with which apoB was associated, we compared the distribution of apoB with that of markers specific for the various steps of the intracellular traffic. PDI and Golgin 97 were used as markers of the endoplasmic reticulum (ER) and Golgi compartments, respectively. Sec-13 was used as a component of the COP-II coat complex, which is associated with the early steps of the ER–Golgi transport process (Klumperman, 2000). We also used β-COP, which is associated with the ER–Golgi and intra-Golgi transport systems as a component of the COP-I coat complex (Kirchhausen, 2000). Figure 2 shows that, in differentiated Caco-2 cells, Sec-13 and PDI were mainly visualized in the subapical (−3 μm) and perinuclear (−6 μm) regions. However, apoB colocalized with Sec-13 and PDI only in the subapical region (Figure 2A, middle). β-COP was found in vesicular structures in the apical, subapical, and perinuclear levels. Most of the β-COP present in the apical/subapical areas colocalized with apoB (Figure 2A, third column, top and middle). By contrast, at the perinuclear level (−6 μm), β-COP staining looked like spread points and did not colocalize with apoB (Figure 2A, third column, bottom). Conversely, the perinuclear pool of apoB was mainly associated with structures corresponding to Golgi vesicles, as shown by its colocalization with the *trans*-Golgi marker Golgin 97 (Figure 2A, fourth column, bottom). We can conclude from the results shown in Figure 2 that apical apoB colocalized with β-COP, whereas subapical apoB colocalized with PDI, Sec-13, and β-COP, and perinuclear apoB colocalized only with Golgin 97.

Because β-COP is a marker of the pre-, per-, and post-Golgi compartments, we identified the compartment containing apical apoB by comparing the distribution of apoB in cells cultured at 37°C or at 19°C for 3 h, post-Golgi vesicular traffic being inhibited at 19°C in enterocytes (Danielsen *et al.*, 1993). We used biotinylation to visualize the BBD instead of SI, the marker used in the previous experiments, because SI traffic is also affected at 19°C. We quantified the apoB-associated fluorescence, relative to the apical localization of biotin labeling, along an apical-to-basal axis, every micrometer. We confirmed that the major pool of apoB was localized in the BBD at 37°C, because apoB maximal fluorescence intensity coincided as a narrow peak with biotin labeling (Figure 2B, dark circles). By contrast, at 19°C, the distribution of the apoB-associated fluorescence broadened out sub-

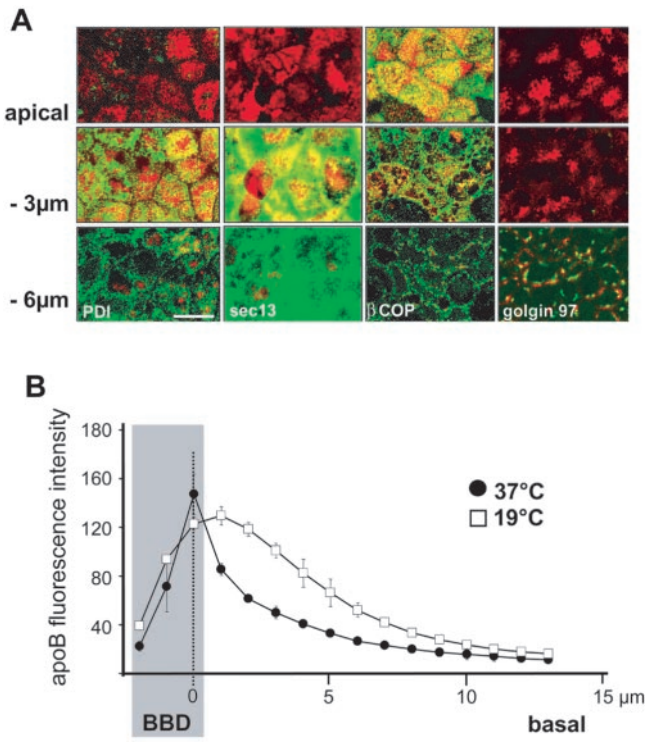

Figure 2. Characterization of apoB-containing subcellular compartments in Caco-2 cells. (A) Immunolocalization of apoB (red channel) at the apex, and 3 μm and 6 μm below the apical plane in Caco-2 cells, compared with that for PDI (endoplasmic reticulum), sec13 (COPII vesicles), β-Cop (COPI vesicles), and Golgin 97 (*trans*-Golgi) (green channels). Bar, 10 μm. (B) Effect of temperature on the distribution of apoB; cells were cultured at 37°C or 19°C for 3 h. The localization of apoB was determined by confocal microscopy with respect to the apical domain (BBD, gray area), which was labeled with nonpermeant reactive biotin (sulfo-NHS-Biotin) detected with tetramethylrhodamine B isothiocyanate-conjugated streptavidin. For each area that was analyzed, point zero corresponds to the maximal intensity of the biotin labeling of the brush-border membrane (dashed line). The graphs represent the intensity of apoB-associated fluorescence that was evaluated for 12 areas composed of nine to 11 cells at 1-μm intervals along the Z-axis in the BBD and from point 0 to the basal part of the cells.

apically (Figure 2B, open squares). The increase in the apoB signal in the subapical and the perinuclear regions (Figure 2B, 1–6 μm) at 19°C indicated that apoB could not be transported to its apical position at this temperature (Figure 2B, open squares). This experiment supports that, at 37°C, apoB is targeted to the apex after leaving the TGN. Accordingly, the apical apoB visible after 3 h at 19°C most likely left the TGN before the temperature shift and was kept in an apical position because post-TGN exchanges are also considerably reduced at 19°C.

Constitution of the Apical Pool of apoB Depends on Lipid-mediated Export from the ER

Interestingly, apoB did not display an apical distribution if Caco-2 cells were continuously cultured in a serum-free/lipid-free defined medium (ITS) (Figure 3). In these culture conditions, only a small proportion of apoB colocalized with the brush-border–associated SI (Figure 3, A and B, top). apoB was mostly retained in the ER and colocalized with PDI at the subapical level (Figure 3B, left, -3 μm and XZ projection). We saw no retention of apoB in the Golgi apparatus as shown by the lack of increase in colocalization with Golgin 97 (Figure 3B, right column, bottom). Lipid supplementation of ITS medium (0.4 mM oleic acid, 0.2 mM palmitic acid and 0.04 mM cholesterol bound to 1% BSA) (ITS/L) restored the apical distribution of apoB (Figure 3A, insets), and its colocalization with SI, as observed in conditions of serum supplementation (Figure 3A). Single species of lipids were found to be less efficient than combinations in inducing the apical targeting of apoB (Figure 3A). The dramatic difference in the subcellular distribution of apoB in the presence and absence of lipids was not paralleled by strong variations in the cellular amount of apoB, as observed by Western blot (Figure 4A). To examine recovery over time from the cellular and secreted pools of apoB, pulse-chase experiments were performed in the two extreme conditions, i.e., in the presence of FCS or ITS (Figure 4B). After a 1-h pulse, apoB100 labeling accounted for 65% of the total apoB labeling in ITS condition and 50% in FCS condition, a result very similar to that obtained by Western blot analysis. This apoB100/apoB48 ratio did not change over the chase time in the cellular or secreted pool of apoB (our unpublished data). Over the 3-h chase, the intracellular apoB decreased to 24% of its initial value in ITS condition (100% corresponding to 18,000 $\pm$ 1,700 cpm/mg proteins) and to 38% in FCS condi-

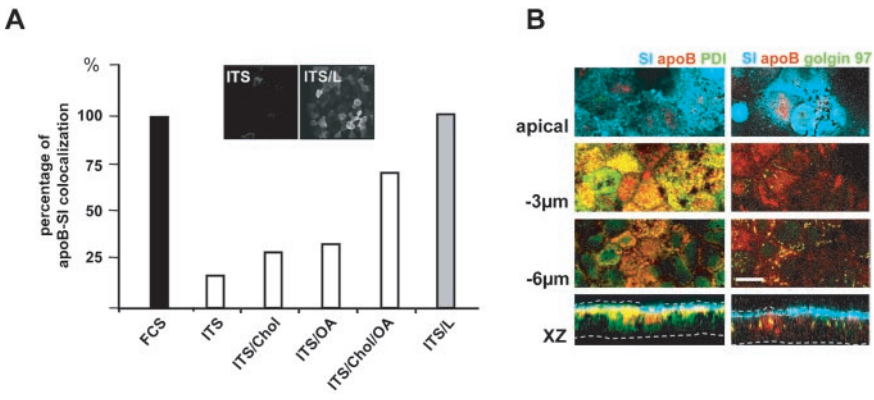

Figure 3. Apical localization of apoB depends on lipid supply. (A) apoB-SI colocalization, as a function of basal lipid supply. In the basal compartment, ITS was used alone or supplemented with oleic acid (OA), cholesterol (Chol), or a mixture of OA, cholesterol, and palmitic acid (ITS/L). Confocal microscopy was used to study the colocalization of SI and apoB in each of these conditions. Results are expressed as the percentage of cells in which apoB and SI colocalized, with the value for cells incubated with FCS-supplemented medium set at 100%. Insets display XY acquisitions of the apoB signal in the apical region of cells cultured with ITS medium alone (ITS) or supplemented with lipids (ITS/L). (B) Immunolocalization of apoB (red channel), SI (blue channel), PDI (green channel on left panel), or Golgin 97 (green channel on right panel) at the apex, and at -3 and -6 μm with respect to the apical plane and in XZ representations in Caco-2 cells cultured in ITS medium. Dotted lines delimit the brush-border domain and the basal level of Caco-2 cells. Bar, 10 μm.

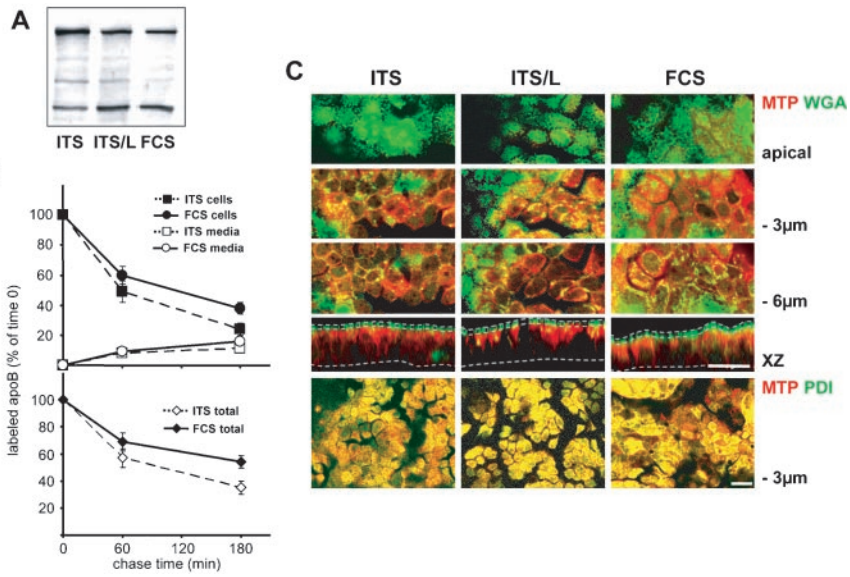

Figure 4. apoB stability and MTP subcellular distribution in the different culture conditions. (A) Western blot analysis of apoB distribution in Caco-2 cells cultured with ITS, ITS/L, or FCS-containing medium in the basal compartment. Forty micrograms of proteins was loaded in each lane. (B) Pulse-chase experiments of apoB in Caco-2 cells cultured with ITS or FCS-containing medium in the basal compartment. After 1 h of labeling with [^{35}S]Met/Cys (0) and at 1 and 3 h of chase, apoB was immunoprecipitated from cell extracts (200 μg of proteins for each condition) and media (250 μl in each condition), electrophoresed, analyzed by fluorography, and counted. Results, from four independent determinations, are expressed as the percentage of labeled apoB recovered in cells and media compared with the 100% amount of labeled apoB at t = 0 of chase, i.e., 18,000 $\pm$ 1,700 and 16,500 $\pm$ 1,300 cpm/mg proteins in ITS and FCS conditions respectively. (C) Confocal analysis of MTP cellular distribution in ITS, ITS/L, and FCS culture conditions. Top, comparison of MTP signal (red channel) and FITC-WGA staining of BBD, Golgi apparatus, and endosomal compartments (green channel) at the apex, and 3 and 6 μm below the apical plane and in XZ representation. Dotted lines delimit the brush-border domain and the basal level of Caco-2 cells. Bottom, immunolocalization of MTP (red channel) and PDI (green channel) at 3 μm below the apical plane. Bars, 20 μm.

tion (100% corresponding to 16,500 $\pm$ 1,300 cpm/mg proteins), whereas the secreted apoB rose to 11 and 16%, respectively. The resulting total recovery from the cellular and secreted pools of apoB was 35 $\pm$ 5 and 54 $\pm$ 4.5% in ITS and FCS conditions, respectively. Therefore, such results indicated that apoB was degraded in Caco-2 cells and also that it was significantly stabilized by the presence of lipids in the culture medium. However, the percentage of apoB that escaped degradation (19%, $p < 0.05$) could not explain by itself the dramatic difference in the localization of apoB between FCS and ITS culture conditions.

Because MTP controls apoB lipidation (Ingram and Shelness, 1997), we then analyzed whether the intracellular distribution of MTP varied according to the different conditions of lipid supply, i.e., in FCS, ITS and ITS/L conditions. The localization of MTP was compared with that of PDI (ER marker) and with FITC-labeled WGA staining. WGA is a lectin, which binds to the external *N*-acetyl glucosamine of oligosaccharide structures and consequently labels the brush-border and basolateral membranes, as well as endosomal and Golgi compartments but not the endoplasmic reticulum. In all conditions, MTP was found localized in ER compartments (Figure 4C, PDI/MTP colocalizations at -3 μm) and, more faintly, in the Golgi apparatus (Figure 4C, WGA/MTP colocalizations at -6 μm). We did not observe the presence of MTP in the BBD whatever the lipid-supplementation condition (Figure 4C). Overall, the subcellular distribution or intensity of MTP was not influenced by lipid supplementation in the basal compartment.

Fatty Acid (FA) Incorporation and Triacylglycerol (TAG) Traffic after Apical Supply of Lipid Micelles

Before analyzing the effect on apoB traffic of apical applications of dietary lipids, we followed the fate of FAs supplied as a complex lipid emulsion, which mimicked the lipid content of duodenum after a fat meal (Hernell *et al.*, 1990) and contained oleic acid (0.6 mM), lysophosphatidylcholine (0.2 mM), cholesterol (0.05 mM), 2-monooleylglycerol (0.2 mM), and taurocholic acid (2 mM). These concentrations of micelle components were not cytotoxic (our unpublished data). Trace amounts of a fluorescent-labeled fatty acid (Bodipy), which is known to be incorporated into TAG and the phospholipids of living cells in a similar manner to long-chain FAs (Elsing *et al.*, 1995), was added to lipid micelles. Bodipy fluorescence, which is associated with newly absorbed lipids, was initially detected as faint diffuse points in the subapical region within the first 15 min (our unpublished data). The intensity of this punctuate staining at the apical and subapical levels increased only moderately over the 60-min period of incubation with micelles (Figure 5A, apical and -3-μm panels). By contrast, from 30 min of incubation, large (0.2–0.5 μm in diameter) intense fluorescent droplets were visualized at -6 μm (Figure 5A), and the number and intensity of these droplets still increased after 60 min in the presence of micelles. Treatment of the cells with nocodazole, an inhibitor of microtubule polymerization, prevented the formation of these lipid droplets (Figure 5A, bottom), indicating that TAG traffic involves the microtubule network.

A similar pattern of change over time was observed if neutral lipids (e.g., TAG and cholesterol esters) were stained with Nile Red (Figure 5B). A small number of neutral lipid-containing droplets (yellow color) were already present in some cell islets before the addition of lipid micelles (our unpublished data), resulting from the endogenous metabolism of fatty acids taken up from basal serum. However, both the number and fluorescence intensity of lipid droplets increased after the addition of micelles, mostly at -6 μm (Figure 5B, yellow color). The similar distributions of bodipy and Nile Red fluorescence strongly suggest that this pool of TAG originates from de novo synthesis from apically absorbed FAs. The formation of lipid droplets occurred in the subapical compartment, within the ER, as visualized by transmission electron microscopy 15 min after the apical supply of lipid micelles (Figure 5C). Lipid droplets were never observed in the apical BBD (Figure 5C), even very early (5 min) after the addition of micelles (our unpublished data). Biochemical analyses confirmed that most of the ab-

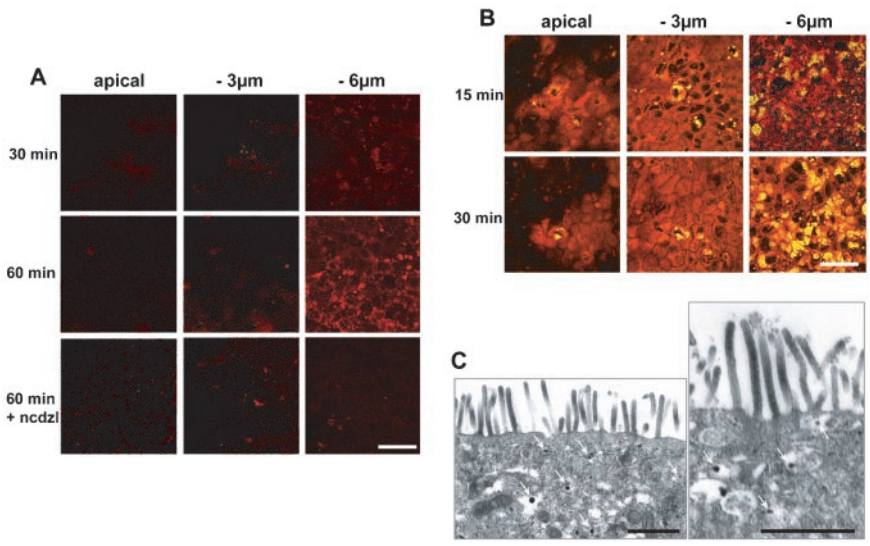

Figure 5. FA incorporation and TAG traffic after the apical application of micelles. Complex lipid micelles were applied apically to Caco-2 cells. (A) micelles contained Bodipy-labeled fatty acids. Bodipy-associated fluorescence was monitored at the apical plane and at 3 and 6 μm below this plane. Cells treated with nocodazole (ncdzl) during the period of incubation with micelles were analyzed after 60 min (bottom). Bar, 50 μm. (B) Accumulation of TAG as assessed by Nile-Red yellow fluorescence after the apical delivery of micelles (red color corresponds to phospholipids). Bar, 50 μm. Note that the kinetics of intracellular traffic were similar for FAs incorporated from micelles and Nile Red stained-TAG. (C) Transmission electron microscopy analysis of lipids localization in Caco-2 cells, 15 min after micelles application. Arrows indicate the presence of lipid droplets in the subapical compartment within the ER (stars). Note that the BBD is devoid of lipid droplets. Bars, 1 μm.

sorbed FAs (50%) was esterified in TAG after 120 min in the presence of lipid micelles.

Apical Supply of Lipid Micelles Results in the Emptying of the Apical Pool of apoB

We investigated whether the apical supply of lipid micelles induced vesicular traffic of apoB concomitant with that of TAG. As soon as 15 min after the addition of micelles, apoB was observed in the vicinity of the lateral membranes, at -6 μm, and the apical pool of apoB was found depleted (our unpublished data). After 30 and 60 min, the pool of apoB at -6 μm was still increasing, and the apical pool had been partly replenished (Figure 6A and XZ representation in inset). Micelle-induced apoB vesicular traffic involved the microtubule network, as did that of TAG, because nocodazole completely inhibited the increase in the lateral pool of apoB (Figure 6B). This traffic depended specifically on complex micelles, because the apical application of an equal amount of oleic acid bound to albumin, the plasma carrier of fatty acids, resulted in only low levels of apoB redistribution, even after 60 min (Figure 6C). Furthermore, the colocalization of apoB with Golgin 97 at the perinuclear level was not modified by the addition of micelles (Figure 6F). The changes in apoB distribution after the addition of micelles were not accompanied by changes in the cellular amount of apoB, as shown by Western blotting on Caco-2 cells cultured in FCS medium with or without apical micelles application (Figure 6D). Results from pulse-chase experiments showed that the apical supply of micelles did not change the cellular amount of apoB but doubled the percentage of the secreted pool of apoB after 3 h of chase. The resulting significant 17% increase in the total recovery of apoB was therefore essentially due to the amount of apoB protected from degradation, which was directed to secretion in the presence of micelles (Figure 6E).

Although our results strongly suggest that the apoB mobilized after the apical delivery of micelles was derived from the apical pool, we could not exclude the possibility that some of the apoB mobilized was derived from a newly synthesized, ER-associated, pool of apoB. Indeed, we showed that apoB was continuously synthesized and targeted to the apical domain. We therefore analyzed apoB traffic after cycloheximide (CHX) treatment, which totally inhibits protein synthesis in Caco-2 cells within 15 min (our unpublished data). In the absence of apically supplied micelles, CHX treatment led to a major increase in the BBD-associated apical pool of apoB colocalized with SI within 60 min (Figure 6G, top). This increase was due to the completion of apoB traffic that was already underway when CHX was added. The apical application of micelles dramatically chased this preexisting apical pool of apoB, which was transported to the subapical and lateral areas before secretion. Consequently, apoB ceased to colocalize with SI in 80% of the cells (Figure 6G, bottom). Similar results were obtained regardless of whether the cells were cultured with FCS- or ITS/L-supplemented medium in the basal compartment (our unpublished data).

Lipids Induce an Up and Down Traffic of apoB in Enterocytes

Because cells cultured in basal FCS or ITS/L-containing medium had a preformed apical pool of apoB before the addition of micelles, we investigated the effects of applying micelles to cells cultured in lipid-deprived ITS medium, in which apoB is mainly retained in the subapical ER (Figure 7A, left). Thirty minutes after the application of micelles, apoB was observed at two main positions: at -3 μm, in a subapical pool in which colocalization with PDI had considerably decreased (Figure 7A, top, 30 min) and at -6 μm under the apical level (Figure 7A). The subapical pool increased in size after 60 min, and this increase coincided with the appearance of an apical pool of apoB in the BBD (Figure 7A, merge signal, XZ panel, 60 min). At this time point, we observed no change in the perinuclear pool of apoB and in its colocalization with the Golgi marker Golgin 97 (our unpublished data). Results from pulse-chase experiments showed that micelles application induced a slight stabilization of the cellular apoB (6%) and doubled the percentage of the secreted apoB after 3 h of chase, resulting in a significant 21% increase of the total recovery from the cellular and secreted apoB (Figure 7B) in the presence of micelles. It must be emphasized that lipid micelles did not induced a significant increase in the biosynthesis rate of apoB (16,500 $\pm$ 900 cpm/mg proteins versus 18,000 $\pm$ 1,700 cpm/mg proteins in the absence of micelles) after the 1-h pulse, i.e., over the

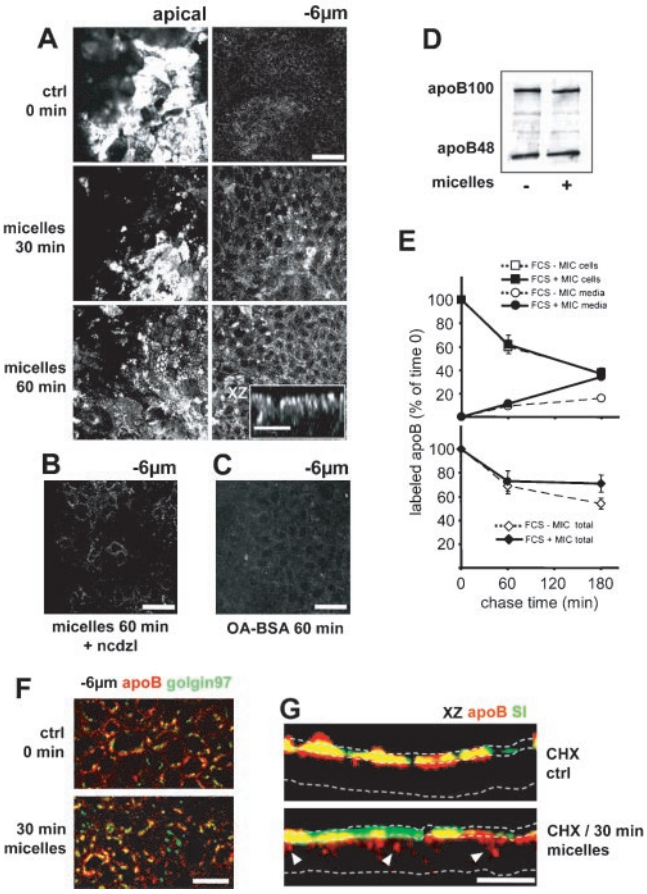

Figure 6. apoB traffic after the apical application of micelles. (A) apoB immunolocalization at the apex and 6 μm below the apex, 30 and 60 min after the addition of lipid micelles; the inset in the bottom panel represents an XZ projection of the XY acquisitions 60 min after micelle delivery. (B) apoB immunolocalization 6 μm below the apex 60 min after micelles delivery in the presence of nocodazole (ncdzl). (C) apoB immunolocalization 6 μm below the apex 60 min after the addition of BSA-complexed oleic acid (OA-BSA). Bars, 50 μm; for inset in A, 10 μm. (D) Western blot analysis of apoB distribution in Caco-2 cells cultured with FCS-containing medium in the basal compartment in the presence (+) or the absence (−) of apical micelles supply. Forty micrograms of proteins were loaded in each lane. (E) Pulse-chase experiments of apoB in Caco-2 cells cultured with FCS-containing medium in the basal compartment in the presence or absence of apical micelles supply. After 1 h of labeling with [^{35}S]Met/Cys (0) and at 1 and 3 h of chase, apoB was immunoprecipitated from cell extracts (200 μg of proteins for each condition) and media (250 μl in each condition), electrophoresed, analyzed by fluorography, and counted. Results, from four independent determinations, are expressed as the percentage of labeled apoB recovered in cells and media compared with the 100% amount of labeled apoB at t = 0 of chase, i.e., 15,700 ± 850 and 16,500 ± 1,300 cpm/mg proteins in the presence or absence of apical micelles supply respectively. (F) Immunolocalization of apoB (red channel) and Golgin 97 (green channel) 6 μm below the apical plane in Caco-2 cells without (top) or with lipids micelles in the medium for 30 min (bottom). Bar, 10 μm. (G) XZ representations of apoB (red channel) and SI (green channel) immunolocalization in Caco-2 cells treated with CHX without (top) or with (bottom) incubation with lipids micelles for 30 min. Dotted lines delimit the brush-border domain and the basal level of Caco-2 cells in the XZ representation. White arrowheads indicate delocalized apoB. Bar, 20 μm. Note that the apical application of micelles specifically induced rapid vesicular traffic of apoB from apical to lateral perinuclear areas.

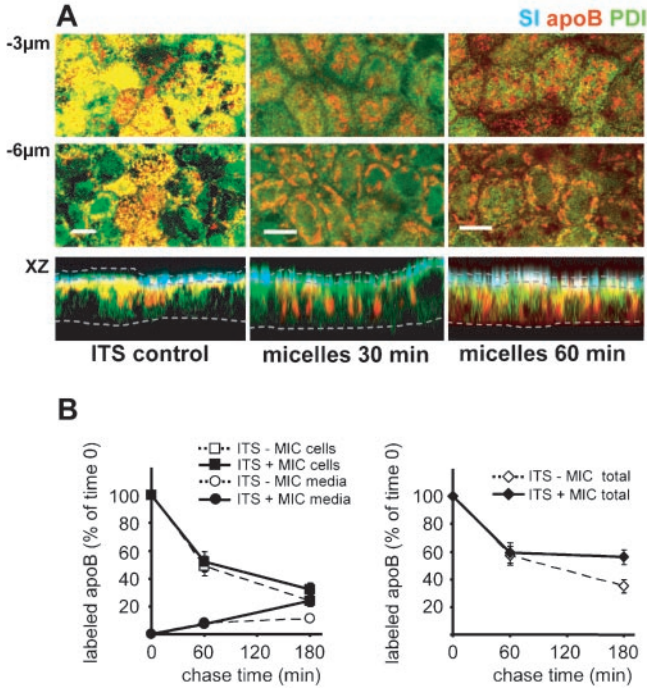

Figure 7. The delivery of micelles to Caco-2 cells cultured in ITS medium induces the export of apoB from the ER and the completion of its traffic. (A) Immunolocalization of apoB (red channel), SI (blue channel) and PDI (green channel), at 3 μm and 6 μm below the apical plane and in an XZ representation of Caco-2 cells cultured in ITS medium before (ITS control) and after 30 and 60 min of incubation with micelles. Dotted lines delimit the brush-border domain and the basal level of Caco-2 cells in the XZ representation. Bars, 10 μm. (B) Pulse-chase experiments of apoB in Caco-2 cells cultured with ITS-containing medium in the basal compartment in the presence or absence of apical micelles supply. After 1 h labeling with [^{35}S]Met/Cys (0) and at 1 and 3 h of chase, apoB was immunoprecipitated from cell extracts (200 μg of proteins for each condition) and media (250 μl in each condition), electrophoresed, analyzed by fluorography, and counted. Results, from four independent determinations, are expressed as the percentage of labeled apoB recovered in cells and media compared with the 100% amount of labeled apoB at t = 0 of chase, i.e., 16,500 ± 900 and 18,000 ± 1,700 cpm/mg proteins in the presence or the absence of apical micelles supply, respectively.

period where the micelles-induced variations in the subcellular localization of apoB were observed.

We investigated the kinetics of formation for the apical and subapical apoB pools by comparing the effects of apical micelles application on BBD-associated apoB in cells cultured in ITS or ITS/L medium. We did this by estimating the percentage of cells in which apoB and SI colocalized apically. In cells cultured in ITS/L medium, the kinetics of apoB traffic after the supply of micelles was similar to that in cells cultured with FCS (Figure 6A): an emptying of the apical pool of apoB within 15 min followed by its replenishment after 60 min. Interestingly, the addition of micelles to cells cultured in lipid-free ITS medium initially induced the replenishment of the apical pool of apoB (Figure 8, up). However, this apical pool was smaller than that observed in cells cultured in the presence of ITS/L or FCS before micelle delivery, and this may reflect the equilibrium between apoB arriving at the apex and transported from the apex in response to micelles application. A decrease in this apical pool of apoB was observed after 30 min (Figure 8, down), later

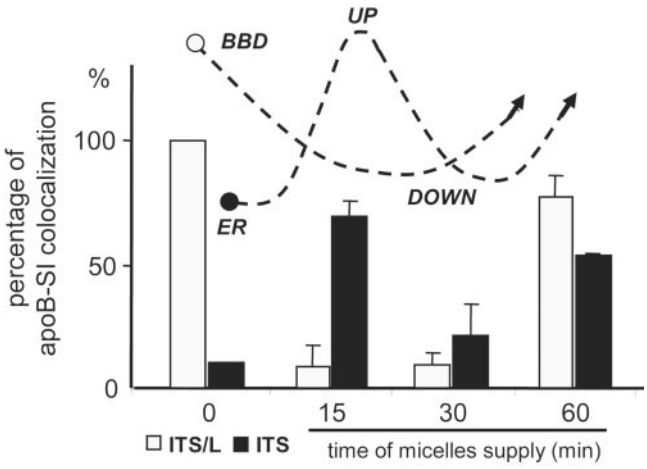

Figure 8. Dynamics of the traffic of the BBD-associated pool of apoB after the delivery of micelles. The colocalization of SI and apoB was analyzed by confocal microscopy 15, 30, and 60 min after the apical application of micelles to cells previously cultured without (ITS) or with (ITS/L) lipids in the basal compartment. Results are expressed as the percentage of cells in which SI and apoB colocalized, the value for ITS/L condition at time 0 being set at 100%. Results are the means for 3 fields of 4×10^4 μm^2 from 2 independent cultures. The curves with dashed lines indicate intracellular apoB traffic. Note that in cells previously cultured in the absence of lipids (ITS), the application of micelles induced the apical targeting of apoB (up) before its chase (down).

than in cells incubated with ITS/L or FCS. Finally, the de novo synthesis and lipid-dependent BBD targeting of apoB replenished the apical pool within 60 min in both conditions.

DISCUSSION

Our results provide a dynamic insight into the enterocyte-specific polarized traffic of a secretory protein, apoB, and its dependence on lipids. We demonstrate that mature apoB accumulates in the apical BBD as "ready-to-use" stores. A supply of lipids is required to ensure the export of apoB from the ER and its subsequent post-Golgi targeting to the apex. An apical application of micelles, which mimic the composition of duodenal micelles resulting from the digestion of dietary lipids in vivo, signals the chase of the apical pool of apoB toward the basolateral areas of the cell, whereas newly synthesized TAG droplets are formed concomitantly from micelles lipids within the ER in the subapical compartment.

Lipid-dependent Formation of the Apical Pool of apoB

In polarized enterocytic Caco-2 cells, we observed a major apical pool of apoB spanning the BBD and the subapical compartment (SAC) (Figure 1). Such a polarized distribution of apoB is cell specific and has never been observed in liver cells, the other site of apoB production, in studies on parenchymal liver cells (Alexander *et al*., 1976) or cultured hepatic HepG2 (Bostrom *et al*., 1988) or McA-RH7777 cells (Boren *et al*., 1994). In both the apical and subapical domains of Caco-2 cells, apoB displayed partial colocalization with β-COP (Figure 2). The apical pool of apoB was derived from the TGN because the inhibition of the post-Golgi vesicular traffic by incubation at 19°C blocked the apical targeting of apoB resulting in its retention in upstream compartments of vesicular traffic.

Our results demonstrate that, in enterocytes, lipids control the export of apoB from the ER and its further targeting toward the apex. This is of physiological importance because the exit of apoB from the ER has also been defined as the limiting step in TRL traffic in enterocytes (Mansbach and Nevin, 1998; Cartwright *et al*., 2000; Siddiqi *et al*., 2003). If polarized Caco-2 cells were cultured in a lipid-free defined medium, apoB accumulated in the ER and its apical targeting was impaired (Figure 3), whereas association of SI with the BB membrane was not affected (Figure 3; Jumarie and Malo, 1991). Conversely, the apical pool of apoB was replenished after the supplementation of basal ITS medium with BSA-bound oleic and palmitic acids and cholesterol (Figure 3) or after the apical application of lipid micelles to cells cultured in lipid-deprived ITS medium (Figures 7 and 8). In hepatocytes, palmitoylation (Zhao *et al*., 2000) and an early, MTP-dependent, lipidation step (Ingram and Shelness, 1997; Fisher and Ginsberg, 2002) are necessary for the stabilization of the newly synthesized apoB as a primordial lipoprotein. Impaired lipidation results in an ER-associated degradation of apoB in hepatocytes, a process mediated by the proteasome complex (Fisher *et al*., 1997; Yao *et al*., 1997; Davidson and Shelness, 2000). The control of intestinal apoB degradation by the same mechanisms is still under debate. No such degradation was reported in Caco-2 cells (Liao and Chan, 2000). Conversely, a degradation of apoB, which was modulated by the nutritional status, was observed by Haidari *et al.* (2002) in hamster enterocytes. They showed that the insulin resistance syndrome of fructose-fed hamsters was accompanied with increases in enterocyte apoB48 amount, MTP activity and de novo synthesis of triglycerides, which suggest that insulin controls apoB degradation in enterocytes as in hepatocytes (Haidari *et al*., 2002). Our results showed that apoB degradation occurs in Caco-2 cells and that the addition of lipids decreases the degradation rate (Figures 4, 6, and 7). We did not observe any obvious modification of the intracellular distribution and intensity of MTP in the different conditions of lipid supply. Thus, providing lipids are supplied to the cells, the MTP-dependent lipidation step of apoB can occur, leading to the formation of primordial lipoproteins and protecting apoB from degradation. MTP being never observed in the BBD (Figure 4), it is obvious, as suggested by Hussain *et al.* (2001) that apoB-containing primordial lipoproteins are formed inside the ER, where we detected the major intensity of MTP and then exit this compartment to be targeted to the BBD.

Our results raise questions concerning the mechanisms by which lipids further control the apical targeting of apoB. Lipid binding may conceal or unmask specific targeting domains in the apoB molecule, such as N-linked glycans and palmitoylated or phosphorylated sites. It must be emphasized that, beyond their effects on this particular TAG-binding protein, lipids have been shown to influence more generally the functional properties of the vesicular compartments involved in protein traffic (McMaster, 2001; Nelson and Yeaman, 2001). Indeed, lipid metabolism participates in the regulation of vesicle transport by controlling SNARE-dependent membrane fusion (Lang *et al*., 2001) and acylation-dependent membrane fission (Weigert *et al*., 1999). Lipid metabolism has also been shown to activate the PI3 kinase signaling pathway, which regulates Golgi-mediated vesicle transport (Roth, 1999), and palmitic acid has been shown to antagonize insulin signaling via Akt/PKB in muscle cells (Storz *et al*., 1999). Further studies have to determine which of these potential mechanisms may account for the control of apoB traffic by lipids in enterocytes.

In accordance with the reported heterogeneity of the SAC (Van and Hoekstra, 1999; Van *et al.*, 2000), our data show that the SAC is an important site in the orientation of apoB traffic. Indeed, in the subapical zone, at -3 μm, we observed the presence of PDI, sec13, and β COP (Figures 2A, 3B, and 7) with which apoB colocalized differently according to the conditions of lipid supply. apoB, therefore, seems to be a valuable tool for deciphering the role of the SAC subcompartments.

Lipid-dependent Recruitment of the Preformed Apical Pool of apoB after the Application of Micelles

It is tempting to consider the BBD-associated pool of apoB as a stock of primordial lipoproteins ready to use in the assembly of apoB-containing TAG-rich lipoproteins by enterocytes after the arrival of dietary lipids via the lumen. The cost of maintaining the apical pool of apoB in enterocytes may be justified as a means of rapidly dealing with the influx of dietary lipids after a meal. Glickman and coworkers observed that apoB was dispersed in the intestinal mucosa of lipid-fed rats, whereas apoB was apically distributed in fasted and bile-diverted rats (Glickman *et al.*, 1976; Glickman *et al.*, 1978). Our present results, in a dynamic enterocyte model, demonstrate that the apical supply of micelles induces the traffic of newly synthesized TAG (Figure 5) and the emptying of the apical pool of apoB together with the appearance of apoB (Figure 6) and lipid droplets (Figure 5) along the secretory pathway. Nocodazole inhibited both apoB and TAG traffics, demonstrating that they require a microtubule-dependent vesicular transport. By treating the cells with cycloheximide, we were able to follow the fate of a synchronized pool of apoB and to demonstrate that the apoB found in lateral areas of the cells after the apical application of micelles originated from the BBD-associated preformed pool (Figure 6). The signal for the rapid chase of the apical pool of apoB was specifically induced by micelles and was not reproduced or, at best, was considerably delayed if fatty acids bound to BSA were applied apically.

Although traffic of both apoB and TAG occur concomitantly, lipid droplets were not observed in the BBD 15 min after micelles application, but rather, as expected, in the SAC within the ER (Figure 5C). Therefore, one can assume that, under micelles application, micelles lipids are used for TAG neosynthesis in the ER and processing of the lipid droplet along the secretory pathway until it assembles with the apoB, which was signaled by micelles to chase down from its BBD post-Golgi stores. This dynamic model of lipid-dependent traffic of apoB in enterocytes could explain the apparent contradictions between morphological observations of the apoB subcellular distribution in the intestine at different steps of its kinetics (Glickman *et al.*, 1976, 1978).

Our results also demonstrate the enterocyte specificity of this process. In Caco-2 polarized enterocytes, the apical delivery of lipid micelles signals the chase of the post-Golgi pool of apoB from the BBD to be used for lipoprotein assembly within the secretory pathway. These results differ considerably from those reported for the liver during very low-density lipoprotein formation, with small dense apoB-containing particles formed in the lumen of the rough ER and requiring fusion with TAG-rich particles formed separately in the smooth ER lumen for export from the ER (Olofsson *et al.*, 2000). Conversely, studies on resuspended cells isolated from rabbit intestinal villi (Cartwright and Higgins, 1999), in which polarization is not preserved, have shown that apoB-containing lipoproteins are assembled only in the SER (Cartwright and Higgins, 2001), as in hepatocytes and hepatoma cell lines. This discrepancy highlights the importance of cell polarity in the enterocyte-specific traffic of apoB.

A Model of Bidirectional Lipid-dependent Traffic of a Secretory Protein

Our data demonstrate a new lipid-dependent process for the control of a secretory protein traffic. This process requires cell polarization and depends on the mode of lipid delivery to the cell. Interestingly, it is a cell-specific process that enables enterocytes to carry out one of their major functions. A supply of fatty acids and cholesterol is sufficient for the export of apoB from the ER and its subsequent post-Golgi traffic up to the apical BBD where it resides until an apical supply of complex lipid micelles signals its chase down to the basolateral secretory domain. These results open up new perspectives concerning the molecular mechanisms and signaling pathways responsible for the enterocyte-specific bidirectional traffic of secretory proteins.

ACKNOWLEDGMENTS

We thank our colleagues at INSERM U505 and Patrice Codogno (INSERM U504, Villejuif, France) for helpful discussions. The confocal and electron microscopy analyses were performed using the facilities of IFR 58. E.M. is recipient of a fellowship from Ministére National de la Recherche et de la Technologie.

REFERENCES

Abumrad, N., Coburn, C., and Ibrahimi, A. (1999). Membrane proteins implicated in long-chain fatty acid uptake by mammalian cells: CD36, FATP and FABPm. Biochim. Biophys. Acta *1441*, 4–13.

Alexander, C.A., Hamilton, R.L., and Havel, R.J. (1976). Subcellular localization of B apoprotein of plasma lipoproteins in rat liver. J. Cell Biol. *69*, 241–263.

Boren, J., Rustaeus, S., and Olofsson, S.O. (1994). Studies on the assembly of apolipoprotein B-100- and B-48-containing very low density lipoproteins in McA-RH7777 cells. J. Biol. Chem. *269*, 25879–25888.

Bostrom, K., Boren, J., Wettesten, M., Sjoberg, A., Bondjers, G., Wiklund, O., Carlsson, P., and Olofsson, S.O. (1988). Studies on the assembly of apo B-100-containing lipoproteins in HepG2 cells. J. Biol. Chem. *263*, 4434–4442.

Carpentier, A., Taghibiglou, C., Leung, N., Szeto, L., Van Iderstine, S.C., Uffelman, K.D., Buckingham, R., Adeli, K., and Lewis, G.F. (2002). Ameliorated hepatic insulin resistance is associated with normalization of microsomal triglyceride transfer protein expression and reduction in very low density lipoprotein assembly and secretion in the fructose-fed hamster. J. Biol. Chem. *277*, 28795–28802.

Cartwright, I.J., and Higgins, J.A. (1999). Isolated rabbit enterocytes as a model cell system for investigations of chylomicron assembly and secretion. J. Lipid Res. *40*, 1357–1365.

Cartwright, I.J., and Higgins, J.A. (2001). Direct evidence for a two-step assembly of ApoB48-containing lipoproteins in the lumen of the smooth endoplasmic reticulum of rabbit enterocytes. J. Biol. Chem. *276*, 48048–48057.

Cartwright, I.J., Plonne, D., and Higgins, J.A. (2000). Intracellular events in the assembly of chylomicrons in rabbit enterocytes. J. Lipid Res. *41*, 1728–1739.

Christensen, N.J., Rubin, C.E., Cheung, M.C., and Albers, J.J. (1983). Ultrastructural immunolocalization of apolipoprotein B within human jejunal absorptive cells. J. Lipid Res. *24*, 1229–1242.

Danielsen, E.M., Hansen, G.H., and Poulsen, M.D. (1993). Apical secretion of apolipoproteins from enterocytes. J. Cell Biol. *120*, 1347–1356.

Davidson, N.O., and Shelness, G.S. (2000). APOLIPOPROTEIN B: mRNA editing, lipoprotein assembly, and presecretory degradation. Annu. Rev. Nutr. *20*, 169–193.

Delie, F., and Rubas, W. (1997). A human colonic cell line sharing similarities with enterocytes as a model to examine oral absorption: advantages and limitations of the Caco-2 model. Crit. Rev. Ther. Drug Carrier Syst. *14*, 221–286.

Elsing, C., Winn-Borner, U., and Stremmel, W. (1995). Confocal analysis of hepatocellular long-chain fatty acid uptake. Am. J. Physiol. *269*, G842–G851.

Fisher, E.A., and Ginsberg, H.N. (2002). Complexity in the secretory pathway: the assembly and secretion of apolipoprotein B-containing lipoproteins. J. Biol. Chem. *277*, 17377–17380.

Fisher, E.A., Zhou, M., Mitchell, D.M., Wu, X., Omura, S., Wang, H., Goldberg, A.L., and Ginsberg, H.N. (1997). The degradation of apolipoprotein B100 is mediated by the ubiquitin-proteasome pathway and involves heat shock protein 70. J. Biol. Chem. *272*, 20427–20434.

Glickman, R.M., Khorana, J., and Kilgore, A. (1976). Localization of apolipoprotein B in intestinal epithelial cells. Science *193*, 1254–1255.

Glickman, R.M., Kilgore, A., and Khorana, J. (1978). Chylomicron apoprotein localization within rat intestinal epithelium: studies of normal and impaired lipid absorption. J. Lipid Res. *19*, 260–268.

Haidari, M., Leung, N., Mahbub, F., Uffelman, K.D., Kohen-Avramoglu, R., Lewis, G.F., and Adeli, K. (2002). Fasting and postprandial overproduction of intestinally derived lipoproteins in an animal model of insulin resistance. Evidence that chronic fructose feeding in the hamster is accompanied by enhanced intestinal de novo lipogenesis and ApoB48-containing lipoprotein overproduction. J. Biol. Chem. *277*, 31646–31655.

Harter, C., and Reinhard, C. (2000). The secretory pathway from history to the state of the art. Subcell. Biochem. *34*, 1–38.

Hauri, H.P. (1988). Biogenesis and intracellular transport of intestinal brush border membrane hydrolases. Use of antibody probes and tissue culture. Subcell. Biochem. *12*, 155–219.

Hauri, H.P., Sterchi, E.E., Bienz, D., Fransen, J.A., and Marxer, A. (1985). Expression and intracellular transport of microvillus membrane hydrolases in human intestinal epithelial cells. J. Cell Biol. *101*, 838–851.

Hernell, O., Staggers, J.E., and Carey, M.C. (1990). Physical-chemical behavior of dietary and biliary lipids during intestinal digestion and absorption. 2. Phase analysis and aggregation states of luminal lipids during duodenal fat digestion in healthy adult human beings. Biochemistry *29*, 2041–2056.

Hussain, M.M., Kedees, M.H., Singh, K., Athar, H., and Jamali, N.Z. (2001). Signposts in the assembly of chylomicrons. Front. Biosci. *6*, D320–D331.

Ingram, M.F., and Shelness, G.S. (1997). Folding of the amino-terminal domain of apolipoprotein B initiates microsomal triglyceride transfer protein-dependent lipid transfer to nascent very low density lipoprotein. J. Biol. Chem. *272*, 10279–10286.

Jacob, R., and Naim, H.Y. (2001). Apical membrane proteins are transported in distinct vesicular carriers. Curr. Biol. *11*, 1444–1450.

Jumarie, C., and Malo, C. (1991). Caco-2 cells cultured in serum-free medium as a model for the study of enterocytic differentiation in vitro. J. Cell Physiol. *149*, 24–33.

Keller, P., and Simons, K. (1997). Post-Golgi biosynthetic trafficking. J. Cell Sci. *110*, 3001–3009.

Kirchhausen, T. (2000). Three ways to make a vesicle. Nat. Rev. Mol. Cell. Biol. *1*, 187–198.

Klumperman, J. (2000). Transport between ER and Golgi. Curr. Opin. Cell Biol. *12*, 445–449.

Lang, T., Bruns, D., Wenzel, D., Riedel, D., Holroyd, P., Thiele, C., and Jahn, R. (2001). SNAREs are concentrated in cholesterol-dependent clusters that define docking and fusion sites for exocytosis. EMBO J. *20*, 2202–2213.

Lestavel, S., and Fruchart, J.C. (1994). Lipoprotein receptors. Cell. Mol. Biol. *40*, 461–481.

Levy, E., and Bendayan, M. (2000). Use of immunoelectron microscopy and intestinal models to explore the elaboration of apolipoproteins required for intraenterocyte lipid transport. Microsc. Res. Tech. *49*, 374–382.

Levy, E., Stan, S., Delvin, E., Menard, D., Shoulders, C., Garofalo, C., Slight, I., Seidman, E., Mayer, G., and Bendayan, M. (2002). Localization of microsomal triglyceride transfer protein in the Golgi: possible role in the assembly of chylomicrons. J. Biol. Chem. *277*, 16470–16477.

Liao, W., and Chan, L. (2000). Apolipoprotein B, a paradigm for proteins regulated by intracellular degradation, does not undergo intracellular degradation in CaCo2 cells. J. Biol. Chem. *275*, 3950–3956.

Lippincott-Schwartz, J., Roberts, T.H., and Hirschberg, K. (2000). Secretory protein trafficking and organelle dynamics in living cells. Annu. Rev. Cell Dev. Biol. *16*, 557–589.

Mansbach, C.M., 2nd, and Nevin, P. (1998). Intracellular movement of triacylglycerols in the intestine. J. Lipid Res. *39*, 963–968.

Massey-Harroche, D. (2000). Epithelial cell polarity as reflected in enterocytes. Microsc. Res. Tech. *49*, 353–362.

McMaster, C.R. (2001). Lipid metabolism and vesicle trafficking: more than just greasing the transport machinery. Biochem. Cell Biol. *79*, 681–692.

Naim, H.Y. (2001). Molecular and cellular aspects and regulation of intestinal lactase-phlorizin hydrolase. Histol. Histopathol. *16*, 553–561.

Nelson, W.J., and Yeaman, C. (2001). Protein trafficking in the exocytic pathway of polarized epithelial cells. Trends Cell Biol. *11*, 483–486.

Nickel, W., Brugger, B., and Wieland, F.T. (1998). Protein and lipid sorting between the endoplasmic reticulum and the Golgi complex. Semin. Cell Dev. Biol. *9*, 493–501.

Olofsson, S.O., Stillemark-Billton, P., and Asp, L. (2000). Intracellular assembly of VLDL: two major steps in separate cell compartments. Trends Cardiovasc. Med. *10*, 338–345.

Roth, M.G. (1999). Lipid regulators of membrane traffic through the Golgi complex. Trends Cell Biol. *9*, 174–179.

Siddiqi, S.A., Gorelick, F.S., Mahan, J.T., and Mansbach, C.M., II. (2003). COPII proteins are required for Golgi fusion but not for endoplasmic reticulum budding of the pre-chylomicron transport vesicle. J. Cell Sci. *116*, 415–427.

Storz, P., Doppler, H., Wernig, A., Pfizenmaier, K., and Muller, G. (1999). Cross-talk mechanisms in the development of insulin resistance of skeletal muscle cells palmitate rather than tumour necrosis factor inhibits insulin-dependent protein kinase B (PKB)/Akt stimulation and glucose uptake. Eur. J. Biochem. .*266*, 17–25.

Van, I.S.C., and Hoekstra, D. (1999). The subapical compartment: a novel sorting centre? Trends Cell Biol. *9*, 144–149.

Van, I.S.C., Maier, O., Van Der Wouden, J.M., and Hoekstra, D. (2000). The subapical compartment and its role in intracellular trafficking and cell polarity. J. Cell. Physiol. *184*, 151–160.

Weigert, R., *et al.* (1999). CtBP/BARS induces fission of Golgi membranes by acylating lysophosphatidic acid. Nature *402*, 429–433.

Yao, Z., Tran, K., and McLeod, R.S. (1997). Intracellular degradation of newly synthesized apolipoprotein B. J. Lipid Res. *38*, 1937–1953.

Zhao, Y., McCabe, J.B., Vance, J., and Berthiaume, L.G. (2000). Palmitoylation of apolipoprotein B is required for proper intracellular sorting and transport of cholesteroyl esters and triglycerides. Mol. Biol. Cell *11*, 721–734.